

Online Monitoring of Ring-Opening Metathesis Polymerization of Cyclooctadiene and a Functionalized Norbornene

Alina M. Alb,[†] Pascal Enohnyaket,[†] Jeanette F. Craymer,[‡] Tarik Eren,[‡]
E. Bryan Coughlin,[‡] and Wayne F. Reed^{*,†}

Physics Department, Tulane University, New Orleans, Louisiana 70118, and Polymer Science & Engineering Department, University of Massachusetts, Amherst, Massachusetts 01003

Received September 27, 2006; Revised Manuscript Received November 16, 2006

ABSTRACT: The kinetics and mechanisms involved in the ring-opening metathesis polymerization of 5-norbornene-2-yl acetate (NAC) and cyclooctadiene (COD) in dichloromethane (DCM) were quantified using automatic continuous online monitoring of polymerization (ACOMP). The results yielded time-dependent monomer conversion and the effects of temperature and reactant concentration, evolution of weight-average molecular mass M_w , and intrinsic viscosity $[\eta]_w$. The evolution of the molecular mass was generally consistent with a “living” mechanism in a rapid first phase, where expected target masses for p(NAC) were met, but often revealed a secondary, slight degradative phase. In contrast, p(COD) yielded molar masses far below target values and generally showed a more pronounced degradative phase. These latter two phenomena for p(COD) appear to be symptomatic of a mechanism that shortens chains with concomitant increase in polydispersity. Furthermore, through a combination of M_w , viscosity, and concentration dependencies it was deduced that the slow degradative phase for both p(NAC) and p(COD) is due almost entirely to cross-metathesis reactions. A probabilistic analysis for cross-metathesis supports these assertions. Automatic continuous mixing (ACM) was used to measure second virial coefficients and intrinsic viscosity, and these are consistent with polymers having large solvent domains and strong interactions for p(NAC). In a further application, a second addition of monomer during reactions revealed that no observable termination takes place over time. Results were cross-checked by conventional multidetector gel permeation chromatography (GPC). Ultimately, this method should help in the control of reactions to produce highly specific polymers and architectures.

Introduction

Olefin metathesis has now emerged as a favored synthetic route for a multitude of preparative reactions.¹ Cross-metathesis (CM) and ring-closing metathesis (RCM) are routinely employed in the synthesis of biologically active molecules.² The preparation of precision macromolecules can now readily be achieved via acyclic diene metathesis (ADMET)³ and ring-opening metathesis polymerization (ROMP).⁴ Development of all four categories of olefin metathesis reactions into useful synthetic routes is due in large part to the availability of optimized metathesis catalysts.⁵

The widespread use of ROMP as a robust and efficient means for polymer synthesis has led to investigations on the kinetics and mechanisms of ROMP reactions.^{6–9} The aim of this paper is to bring the analytical power of the recently developed ACOMP method (automatic continuous online monitoring of polymerization reactions) to measure the polymerization kinetics of cyclic olefins, including the evolution of molar mass and intrinsic viscosity of the resulting polymers. It is of immediate interest to quantitatively compare the course of these reactions to the ideal “living” polymerization paradigm and to seek deviations from this due to processes such as interchain cross-metathesis, “backbiting”, and other possible mechanisms.

Automatic continuous online monitoring of polymerization reactions (ACOMP) was introduced in 1998.¹⁰ It is a nonchromatographic technique that requires the continuous withdrawal of a small sample stream from the reactor, which is diluted to the degree that measurements made on the flowing sample are dominated by single particle properties, not by polymer interac-

tions. Typically, combining multiangle light scattering, ultraviolet absorption, viscometry, and differential refractometry allows the determination of monomer conversion and measures of polymer molecular mass. It has been successfully applied to many homogeneous polymerization systems: free radical,¹¹ nitroxide-mediated controlled radical polymerization (CRP),¹² atom transfer radical polymerization (ATRP),¹³ step-growth reactions,¹⁴ simultaneous determination of average composition and mass distributions in free radical and controlled radical copolymerization,^{15,16} and for continuous reactors.¹⁷ Although no chromatographic columns are used, means for obtaining average mass distributions and indices of polydispersity in some cases have been presented.¹⁸

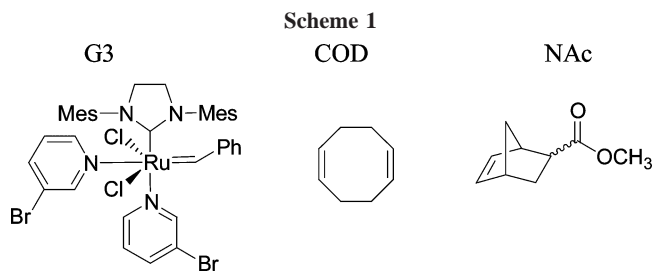
The object of this first time demonstration of ACOMP for monitoring ROMP reactions is to determine how well conversion kinetics and the evolution of M_w and $[\eta]_w$ can be followed and how these compare to the ideal “living” paradigm. Furthermore, it is of interest to establish a means of determining whether termination or transfer reactions occur and whether direct measurements on intra- and/or intermolecular degradative mechanisms can be made. This should clear the way for extension of the methods to diblock synthesis, control of reactions, and monitoring of postpolymerization functionalization reactions.

Materials and Methods

Experimental Conditions. The cyclic olefins 1,5-cyclooctadiene (COD), 5-norbornene-2-yl-acetate (NAC), endo/edo 80:20, Grubbs’ second-generation catalyst (G2), 3-bromopyridine, and ethyl vinyl ether (EVE) were purchased from Aldrich and used as received. Methylene chloride (DCM) was used as received (Fisher) as a solvent for the ring-opening metathesis polymerization, ACOMP

[†] Tulane University.

[‡] University of Massachusetts.



dilution, and GPC elution. Grubbs' third-generation catalyst (G3) was prepared according to the method of Choi and Grubbs¹⁹). Scheme 1 shows the chemical structures of G3 along with the two monomers used in this study. A small stream of the reactor solution was continuously withdrawn by an HPLC Shimadzu LC-ADvp isocratic pump, diluted with solvent (DCM) in a high-pressure mixing chamber and passed at 2 mL/min through the following detectors: a Brookhaven BIM_wA multiangle light scattering detector (MALS), a custom-built single capillary viscometer, a Shimadzu SPD-20 ultraviolet (UV)/visible photodiode array absorption spectrophotometer, and a Waters 410 refractive index (RI) detector.

The reactor contained ~100 mL solution for each reaction, and the starting concentration of monomer in the reactor ranged from 0.2% to 2% by mass. Dilution was normally 50%, except for cases where high initial monomer concentration was used (see Table 1). The delay time from the reactor to the detector train was 30 s (for a 50% dilution), and the response time was 20 s, putting a lower limit on the time scales that could be monitored. This latter was determined by measuring the time the system took from the leading detector edge to stabilization, for any given detector, when a sudden change to the reactor was made, e.g. adding monomer. Interdetector dead volumes were 0.167 mL (5 s at 2 mL/min) from viscometer to MALS and 0.1 mL (3 s at 2 mL/min) MALS to RI. The detector sampling rate was 0.5 Hz.

Automatic Continuous Mixing (ACM). The ACM technique, described in detail in previous work,^{20,21} is used to determine equilibrium properties of multicomponent solutions, such as weight-average molecular mass, M_w , second and third virial coefficients A_2 and A_3 , and weight-average intrinsic viscosity $[\eta]_w$, by forming continuous gradients along chosen paths in composition space. A

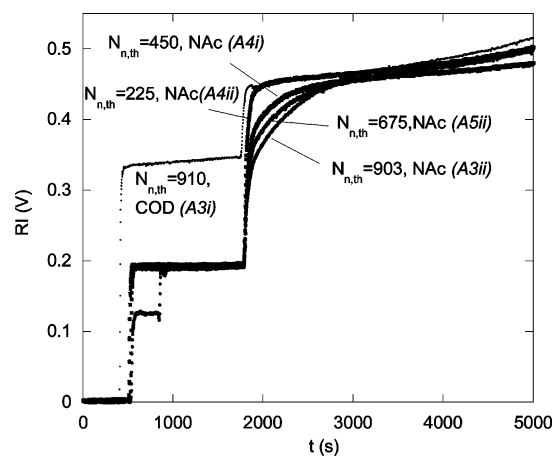


Figure 1. Typical raw RI data for a series of COD and NAC reactions, performed at 1 °C in DCM.

programmable HPLC Shimadzu LC-10ATvp mixing pump was used to pass the solutions through the same detector train used for ACOMP.

Multidetector Gel Permeation Chromatography (GPC). GPC work was carried out using the ACOMP detector train, to which two PLgel individual pore size 5 and 50 μm chromatographic columns connected in series, and an injector with a 0.1 mL loop were added. DCM solvent (same as in ACOMP) passed through the system at 1 mL/min.

By separating monomer from polymer, on discrete, manually withdrawn reaction aliquots, or on samples from the waste stream, GPC allowed a cross-check on the continuous ACOMP conversion and molecular mass data. GPC data were also used to determine polydispersity.

Results

Figure 1 shows typical raw RI data for some of the COD and NAC reactions, performed at 1 °C in DCM, listed in Table 1. The theoretical final value of the number-average degree of polymerization $N_{n,\text{th}}$ is equal to $[\text{NAC}]/[\text{G3}]$ and is given in

Table 1. Reaction Conditions^a

expt	[COD] $\times 10^3$	[NAC] $\times 10^3$	[G3] $\times 10^5$	$N_{n,\text{th}}^{\text{d}}$ $N_{w,\text{ex}}$	expt	[COD]	[NAC]	$C_{m,\text{det}}$ (g/cm ³) $\times 10^3$	[G3] $\times 10^5$	$N_{n,\text{th}}^{\text{d}}$ $N_{w,\text{ex}}$
A1i ^b	25.7		5.13	500	C1ii*	0.268		2.897	37.38	717
				NA ^e	RT					20
A1ii ^b	25.9		2.93	890	C2	0.518		5.611	69.74	744
				NA	RT					80
A2 ^b	25.96		1.72	1510	C3	0.518		5.611	36	1440
				NA	RT					88
A3i ^b	51.9		5.72	910	C4	0.136		1.473	38	403
				NA	RT					15
A3ii		37	4.12	903	C5	0.258		2.713	52.27	480
				914	5 °C					8
A4i		37	8.25	450	C6i		0.734	5.547	16.30	450
				460	1 °C					330
A4ii		37	16.5	225	C7i		0.073	2.777	14.46	508
				272	1 °C					NA
A5i		37	11.00	337.5	C7ii		0.143	2.705	28.57	500
				385	1 °C					NA
A5ii		37	5.50	675	C7iii		0.147	1.698	28.84	510
				670	1 °C					NA
A6ii ^c		37	5.5	450	C8ii		0.146		32.05	457
		75 ^c	8.19 ^c	920 ^c	1 °C					460
A7i		37	8.25	450	C9ii		0.146		23.11	634
				445	25 °C					600
				C10		0.253		4.0153	32.89	768
				RT						760

^a Temperature at which reactions A are made was 1 °C. Dilution in detector train was 50% for these reactions. Reactions C are done on high concentration solutions. Theoretical final values for N_n ($N_{n,\text{th}}$) are shown together with the experimental final values of N_w ($N_{w,\text{ex}}$). ^b No LS change due to dilution of reactor solution \rightarrow LS data cannot be used. ^c Extra monomer added. ^d $N_{n,\text{th}} = [\text{monomer}]/[\text{G3}]$. ^e NA = not available.

Table 2. dn/dc Values for Monomers and Polymers in DCM

NAc ($m = 151.2$ g/mol)	p(NAc)	COD ($m = 108.2$ g/mol)	p(COD)	G3
$0.050 \pm 3\%$	$0.118 \pm 5\%$	$0.083 \pm 5\%$	$0.114 \pm 4\%$	0.173

Figure 1 for each experiment and in Table 1. The DCM baseline runs until 500 s, at which point the monomer is added. The quick response to the addition is seen in the signal jump. The plateau height allowed for computation of dn/dc for COD and NAc (Table 2 gives dn/dc for monomers and polymers). At 1900 s the G3 catalyst was added. The subsequent increase in the RI signal was due to the increased dn/dc of p(NAc) and p(COD) compared to the monomeric form and hence is a direct measure of conversion. While dn/dc is expected to change from its monomeric to long chain polymeric values for short chain lengths, the transition apparently occurs at such low chain lengths that there is no perceptible effect on evaluating conversion kinetics via the RI signal (see below). The contribution to the RI signal from G3 was ascertained from its independently determined dn/dc (Table 2) and found to be negligible for the concentrations of G3 used.

After the initial polymerization phase, there was sometimes an upward drift in the various detectors. This was traced to DCM evaporation due to N_2 purging (DCM bp is $40^\circ C$), leading to small but measurable increases in solute concentration. Later experiments were performed without N_2 , which eliminated the drift, and there were no adverse effects on the polymerization characteristics. In these experiments, the reactor liquid was purged with N_2 for 20 min only at the beginning of the polymerization reaction. This is characteristic of the selectivity of G3, making it robust and eliminating the meticulous gas purging typically required for free radical and controlled free radical polymerizations. G3 is found to initiate reactions more rapidly than G2 and also give lower polydispersity products.^{16,22}

Figure 2 shows LS data at 90° and raw, baseline-subtracted viscosity for typical COD and NAc reactions (C2 and A3ii in Table 1). The increase of both signals marks both the increasing chain length in the living-like ROMP reaction and increased concentration of polymer. Together with the RI-based conversion data M_w can be obtained and is discussed below. Likewise, the viscosity data with the conversion data yield the reduced viscosity η_r . Despite the higher mass concentration of COD than NAc and the fact that *targeted* molar masses were similar, the COD signals are much lower than those for NAc due to the

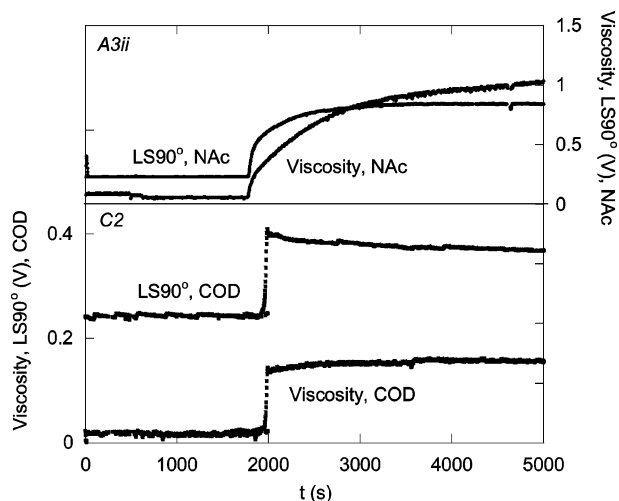


Figure 2. Raw viscosity (after subtracting solvent baseline) and LS data at 90° for typical COD and NAc reactions (C2 and A3ii in Table 1).

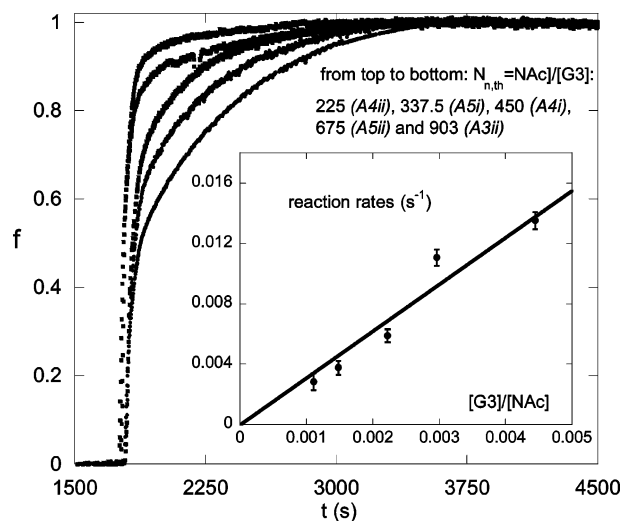


Figure 3. Fractional monomer conversion, f , vs time, based on raw data shown in Figure 1. The inset to figure shows the first-order dependence of the rate constants from these reactions vs $[G3]$.

fact that p(COD) falls far short of the theoretically predicted molar mass.

Figure 3 (corrected for RI drift due to N_2 , in those cases when it occurred) shows monomer conversion kinetics based on raw data shown above, where f represents the fractional monomer conversion. Results can be treated *approximately* as first order over the majority of conversion. Because of the combined response and delay time of about 60 s, the first part of the reaction is unmeasurable, but a sufficient amount is available in all cases for analysis. The 60 s is a mere technical feature of the ACOMP system used here and can be lessened through improved design. The inset to Figure 3 shows excellent linearity of first-order rates with concentration of G3.

Figure 4a shows ACOMP mass evolution vs time for several NAc reactions, and Figure 4b shows M_w vs fractional monomer conversion f . The values of A_2 determined by ACM (Figure 7, described below) were used to correct the values of M_w according to the usual Zimm equation. The M_w vs f behavior is close to the linear expectation. The molar masses of NAc and COD are given in Table 2 to convert between molar masses and degree of polymerization. Also shown on the continuous curve for the $[NAc]/[G3] = 450$ case are discrete points obtained by GPC analysis on manually withdrawn aliquots. The agreement is excellent.

Figure 4b inset shows final M_w from ACOMP for the NAc experiments listed in Table 1 vs $[NAc]/[G3]$ at a fixed value of $[NAc] = 0.0372$ M. The solid black line in the M_w graph is the theoretical expectation for M_n based on monomer/catalyst. The size of the data point solid circles approximately corresponds to the error bars in the M_w measurements. The close agreement between M_w and expected M_n confirms that the NAc reactions closely resemble ideal living polymerization and that the polydispersity is also low.

Figure 5 shows $[\eta]_w$ vs conversion for NAc. Multidetector GPC values for $[\eta]_w$ are also shown for the $[NAc]/[G3] = 450$ case and are in excellent agreement.

In contrast to the living behavior of the NAc reactions, the COD reactions produced polymers far below the theoretically expected $N_{n,th}$, with high polydispersities. The departure from ideality is seen dramatically in Table 1, where both $N_{n,th}$ and the experimental weight-average mass $N_{w,ex}$ (close to N_n for low polydispersity) are shown. Mechanisms for this are discussed

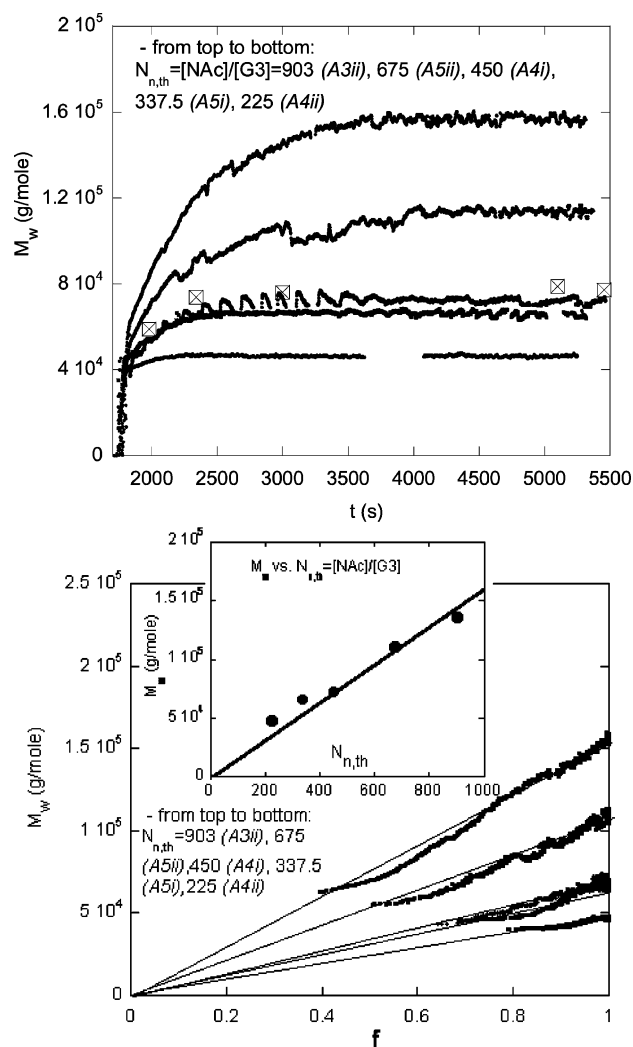


Figure 4. (a) ACOMP mass evolution vs time for several NAC reactions. Discrete, square points are from GPC on manually withdrawn aliquots. (b) M_w vs fractional monomer conversion f . The inset shows final values of M_w . The line is the theoretical expectation for final M_n .

Table 3. GPC Results for Some p(NAC) and p(COD) End Products

	expt	M_w (g/mol)	M_w/M_n
p(NAC)	A7i	77120	1.07
	C8ii	79670	1.09
	C10	145760	1.05
p(COD)	C5	all data	1745
		data without peak 1	2225
		data without peaks 1, 2	3380

below, as well as the pronounced secondary degradation phase measured for p(COD).

GPC Cross-Checks of M_w and $[\eta]_w$ on Reaction Aliquots.

Because ACOMP is still a relatively new method, it is important to cross-check its results with standard methods, of which multidetector GPC is one of the most widely used. GPC also provides polydispersity information that ACOMP does not, making it a valuable complementary method. Aliquots manually withdrawn from NAC reactions A7i and C8ii and end products for several reactions were analyzed using combined MALS and RI data. For GPC on reaction aliquots, Figures 4a and 5 show that M_w for A7i are in excellent agreement with those from ACOMP.

Figure 6 shows the mass distributions for end products of several experiments, determined by the combined MALS and RI data. The polydispersity for the three NAC reactions is low,

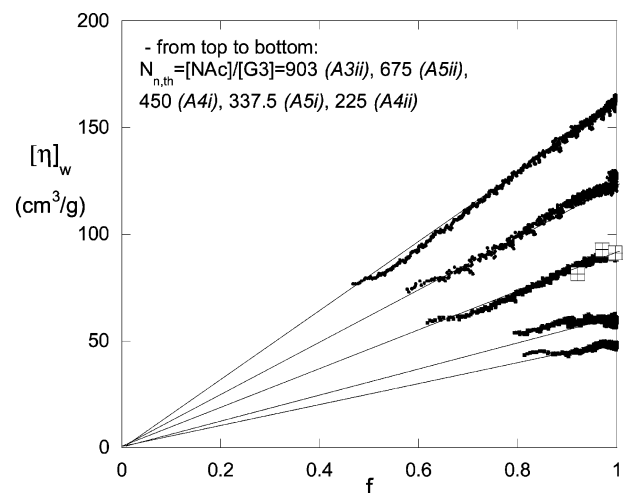


Figure 5. Weight-average intrinsic viscosity $[\eta]_w$ vs conversion for NAC reactions. Discrete, square points are from GPC on manually withdrawn aliquots.

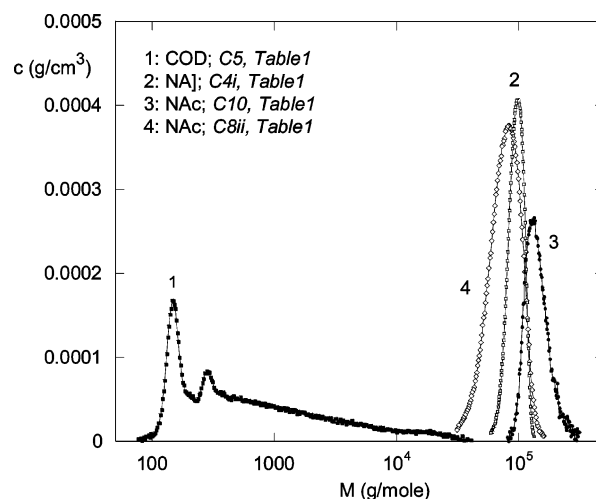


Figure 6. Mass distributions from several NAC and one COD reaction (see Table 1). The failure of COD to produce a living type polymerization is strikingly seen in the low mass peaks and highly smeared out mass distribution.

which is characteristic of a living reaction; i.e., M_w/M_n is less than 1.1, as shown in Table 3. This confirms the ACOMP conclusion that ROMP of NAC is close to an ideal living polymerization.

The strikingly smeared out mass distribution with low mass bimodal peaks for p(COD), also shown in Figure 6, confirms the ACOMP result that anomalously low masses are produced, along with macrocycles, corresponding to the low mass peaks. The data also provide estimated values for the polydispersities, shown in Table 3. Unlike the p(NAC) the p(COD) masses are so low that no usable MALS data was obtained from multidetector GPC, and calibration by polystyrene standards was used for the Table 3 p(COD) values. Excluding the multimodality suggested by the first two peaks for p(COD) in Figure 6, the polydispersity of the smeared out polymer was 2.96, which is very broad and not characteristic of a living polymerization. In connection with the narrow macrocycle peaks, it should be noted that they elute at lower elution volumes than corresponding linear polymers of the same mass, and hence their masses are underestimated when using GPC column calibration methods.

End-Product Characteristics. These were determined both by examining the ACOMP results at the end of each reaction and from ACM data gathered from experiments on end products.

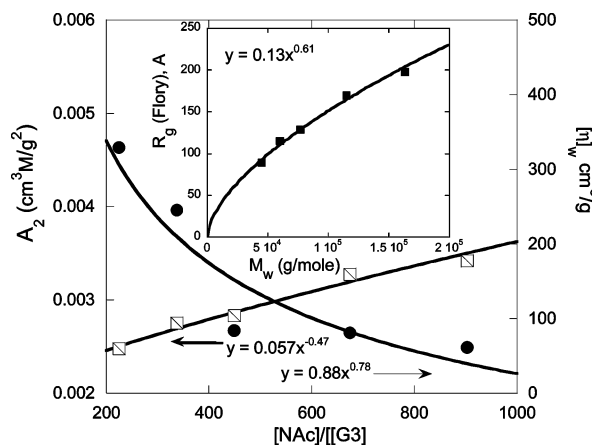


Figure 7. A_2 (solid circles) and $[\eta]_w$ (squares) from ACOMP for NAc reactions. In the inset is $R_{g, \text{Flory}}$ from eq 1.

The ACOMP M_w and $[\eta]_w$ values at final conversion were used in the Flory equation for a coil polymer at Θ -point (no excluded volume) to compute the root-mean-square radius of gyration, $R_g \equiv \langle S^2 \rangle^{1/2}$ for selected p(NAc) samples, shown in Figure 7.

$$[\eta] = \frac{\Phi}{M} (\sqrt{6} \langle S^2 \rangle^{1/2})^3, \quad \Phi = 2.56 \times 10^{23} (\text{mol}^{-1}) \quad (1)$$

Despite the above oversimplification, the power law $R_g = 0.132M^{0.61}$ is in the expected range for a polymer coil in a good solvent and consistent with the strong A_2 and high intrinsic viscosities.

Also shown in Figure 7 are the A_2 values from ACOMP for p(NAc). Using the hard-sphere approximation for the polymer-polymer two-body interaction, an equivalent excluded-volume radius R_{eq} can be found via

$$A_2 = \frac{N_A 16\pi R_{\text{eq}}^3}{3M^2} \quad (2)$$

To obtain an idea of the rigidity of the polymer chains, the apparent persistence lengths L_p' can be computed in the coil limit via the wormlike chain model, where the normally used unperturbed mean-square radius of gyration $\langle S^2 \rangle_0$ is replaced with the perturbed value to obtain L_p' , via^{23,24}

$$\langle S^2 \rangle = \frac{LL_p'}{3} \quad (3)$$

where L is the contour length of the polymer, which was computed from M_w using 23 g/(mol Å) for NAc. $\langle S^2 \rangle^{1/2}$ from the Flory equation R_{eq} obtained by A_2 are remarkably close. The inset to Figure 7 shows the R_g obtained by the Flory equation.

Computation of L_p' averaging over both methods yields $L_p' = 14.0 \pm 0.8$ Å for p(NAc). While this is stiffer than a typical synthetic polymer, it is still quite flexible and indicates that the side group adds only a modest amount of stiffening.

In contrast, analyzing ACOMP values for M_w and $[\eta]_w$ led to an estimate of $L_p' = 3.6$ Å for p(COD). This is considerably more flexible than p(NAc), but within expectation of a mostly freely rotating chain with fixed bond angles.

Assessing Possible Termination Reactions. In order to make a quantitative test of the robustness and durability of G3 and the living nature of the mechanism, a second addition of

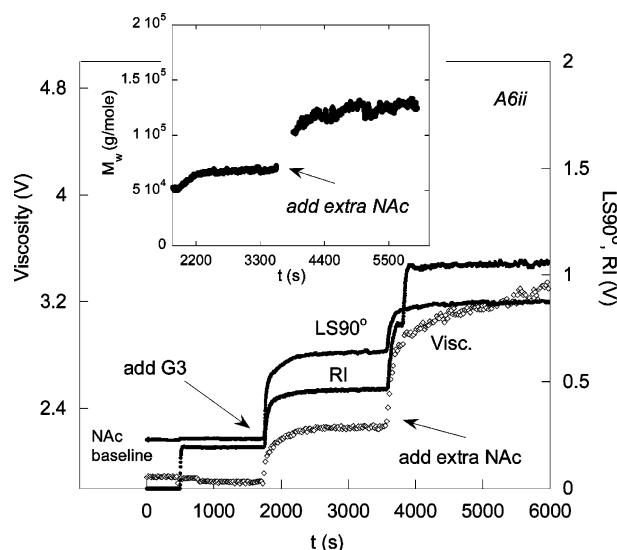


Figure 8. Raw data for experiment A6ii—addition of extra monomer in order to check whether any termination occurs. The inset to figure shows the analysis in terms of M_w .

monomer to the original concentration was made long after the first monomer reached full conversion in several experiments. This monomer addition doubled the initial $N_{n, \text{th}}$. Figure 8 shows an example of this effect (A6ii in Table 1).

The inset to Figure 8 shows the analysis in terms of M_w . The M_w reached is that expected. It can be asserted that no measurable termination of G3 catalyst occurred. This method provides a general, quantitative means for assessing termination.

Effects of Temperature on [NAC] Kinetics. One of the NAc reactions (A5ii, Table 1) was repeated at different temperatures. Experiments carried out at 1, 10, and 25 °C led to a slope of $\ln(\alpha)$ vs $1/T$ of 3720 (1/K), yielding an activation energy of 7.4 kcal/mol or 1.67×10^4 J/mol (α is the first-order rate).

It was reported that increasing the temperature from 23 to 55 °C may result in much broader polydispersity and that chain transfer or backbiting occurs at higher temperatures.¹⁵ However, in this work, p(COD) was obtained with a higher polydispersity even at a reaction temperature of 0 °C. This demonstrates that G3 initiates rapidly, and mechanisms such as cross-metathesis and backbiting are not prevented at low temperatures, at least for the case of COD.

Secondary Degradative Phase; Strong Evidence of Cross-Metathesis. It was generally found that for COD there was a pronounced secondary phase after monomer conversion, where LS decreased yet viscosity remained steady. In contrast, for the case of NAc, there was often no evolution after conversion was complete, or if there was, it was usually far less pronounced than for COD. For NAc there was sometimes a decrease in viscosity accompanying the decrease in LS. Some examples of these effects are shown in Figure 9.

The picture that emerges from the combined ACOMP/GPC data for p(COD) is the following: During the very rapid monomer conversion phase there is a large amount of macrocycle formed due to “backbiting”, which, as an intramolecular mechanism, also occurs rapidly.²⁷ The result is a large accumulation of macrocycles and smeared out distribution of chains, all far below $N_{n, \text{th}}$. The low mass peaks in Figure 6 may be evidence of this low molar mass macrocycle. After this fast conversion phase the polydispersity is very high.

The subsequent, slow degradative phase in Figure 9 is interpreted as interchain cross-metathesis. It appears to be too slow to be important during the very fast initial phase when all

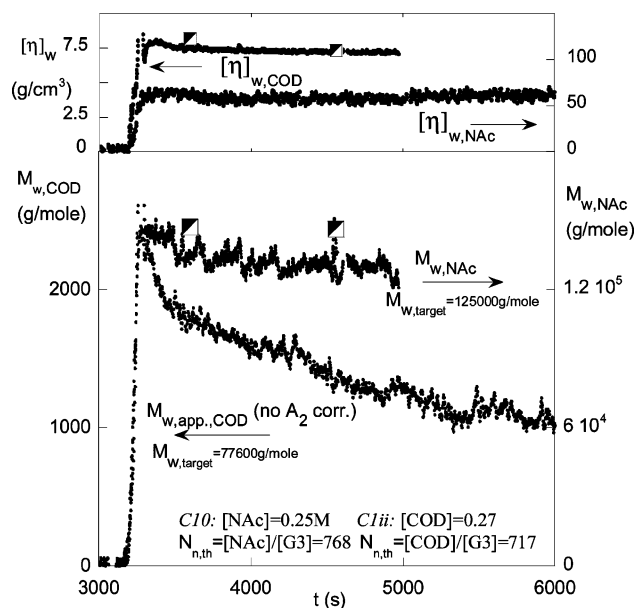


Figure 9. Different long-term trends in M_w and $[\eta]_w$ for COD and NAc reactions (C1ii and C10, Table 1).

monomer is consumed. There was a wide variety of results for the secondary phase, and the variety and complexity of these phases are beyond the scope of this first ROMP-ACOMP work to analyze quantitatively. Rather, some trends are shown in Figure 9 and an initial rationalization is given.

For p(COD) $[\eta]_w$, which is sensitive to a mass average close to M_n , does not change during the degradative phase, whereas LS, which measures M_w , decreases. These raw data trends are consistent with cross-metathesis, as opposed to backbiting.

In cross-metathesis, the G3 on the end of one chain “splices” into a central portion of another chain, while cleaving it. The resulting number of chains does not change; hence, M_n does not change for cross-metathesis but will decrease for backbiting where an intramolecular backbiting event turns one chain into two. Cross-metathesis is consistent with little or no change in viscosity, but the decrease in M_w is a bit more subtle. In fact, if M_w decreases while M_n stays the same, then the polydispersity of the population is *decreasing* due to cross-metathesis.

As noted above, p(COD) produced with G3 is highly polydisperse, consistent with both GPC analysis ($M_w/M_n \sim 3$ for C5), and final masses are far lower than the theoretically predicted ones ($N_{n,th} = 480$, $N_{w,ex} = 8$). There is also usually a strong phase of M_w degradation. These manifestations are symptomatic of chain transfer reactions and high polydispersity.

In contrast, the much smaller secondary degradative effects observed for NAc are consistent with its lower polydispersity and the fact that p(NAc) reaches the theoretically expected values. The fact that p(NAc) shows less metathesis than p(COD) might be explicable on the basis of NAc adhering closer to the living paradigm, as seen by how it meets target masses and shows linear M_w vs conversion evolution.

There are clear precedents for the p(COD) behavior in the literature. Highly active ruthenium systems are reported to not form well-defined polymeric structures for low-strain cyclic olefins.²⁵ The resulting polymers have relatively high polydispersity which suggest that significant chain transfer occurred during the polymerization. The percent trans olefin in the polymer backbone increased with time, indicating that secondary metathesis isomerizations also occur.²⁶ Monitoring by ¹H NMR of the ROMP of COD using Grubbs’ second-generation catalyst

indicated that complete conversion of unreacted initiator to propagating species through chain transfer was observed. During the ROMP of COD significant side reactions can also result, such as cross-metathesis, and measurements of the equilibrium between monomer, cyclic oligomers and polymer have been made.²⁶

Demonstration of How Polydispersity Can Increase or Decrease Due to Cross-Metathesis, Depending on Initial Polydispersity and Distribution. It may seem counterintuitive that polydispersity can increase during a “degradative” reaction. The simplest demonstration of the idea that polydispersity can increase or decrease during cross-metathesis is to consider cross-metathesis of just two initial chains, one with M monomer units the other with N monomer units. One chain, N attacks M , cleaving M into two fragments j and $M - j$. After this, one fragment joins with N , yielding two possible combinations of final chains: (1) $N + M - j$ (each side terminated in ruthenium, Ru) and j (no Ru at all) and (2) $N + j$ and $M - j$ (each terminated with a single Ru).

By definition the starting values of N_n and N_w are

$$N_{n,0} = \frac{N + M}{2} \quad \text{and} \quad N_{w,0} = \frac{N^2 + M^2}{N + M} \quad (4a,b)$$

After one metathesitic exchange with given j , the new N_w is

$$N_{w,j} = \frac{1}{2(N + M)} [(N + j)^2 + (M - j)^2 + (N + M - j)^2 + j^2] \quad (5)$$

This reduces to

$$N_{w,j} = \frac{1}{N + M} [N^2 + M^2 + MN - 2jM + 2j^2] \quad (6)$$

Averaging overall equally likely values of j from 1 to M yields

$$N_w = \frac{1}{M(N + M)} \sum_{j=1}^M [N^2 + M^2 + MN - 2jM + 2j^2] \quad (7)$$

In the limit of long chains, i.e., $M \gg 1$, this can be turned into an integral and integrated, with the result

$$N_w = \frac{1}{N + M} \left[N^2 + MN + \frac{2}{3} M^2 \right] \quad (8)$$

A convenient parametrization is that $M = \alpha N$, where $\alpha \in (0,1)$. M and N play asymmetrical roles in the above equation because N attacks M .

For a given pair of chains of lengths M and N , linked by $M = \alpha N$, however, either chain can attack the other with equal probability, so the proper way to account for this is to take the average of the above expression together with the expression with M and N interchanged. This yields

$$N_w = \frac{1}{2(N + M)} \left[\frac{5}{3} N^2 + 2MN + \frac{5}{3} M^2 \right] \quad (9)$$

or in terms of α

$$N_w = \frac{N}{2(1 + \alpha)} \left[\frac{5}{3} + 2\alpha + \frac{5}{3} \alpha^2 \right] \quad (10)$$

(There is inherent asymmetry of having only one chain scission in the binary encounter; when $N > M$, the attacking chain always ends up $>N$ and $>M$. When $N < M$, the attacking chain ends

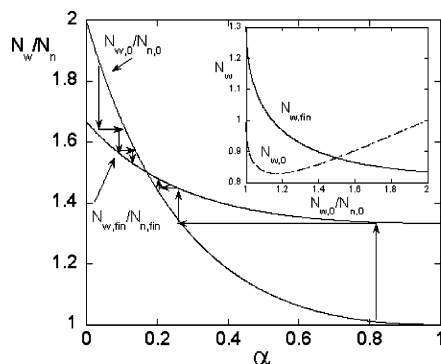


Figure 10. Two cross-metathesitically interacting chains of arbitrary initial lengths M and N will end up at a final polydispersity of $N_w/N_n = 1.5$. If the starting N_w/N_n is greater than this, the polydispersity and N_w decrease during successive interactions, whereas polydispersity and N_w increase if N_w/N_n starts at less than 1.5. The relationship between $N_{w,0}$ and $N_{w,fin}$ as a function of $N_{w,0}/N_{n,0}$ are shown in the inset.

up $> N$ but not necessarily $> M$.) $N_{n,0}$ and $N_{w,0}$ become, in terms of α

$$N_{n,0} = \frac{N(1 + \alpha)}{2} \quad \text{and} \quad N_{w,0} = \frac{N(1 + \alpha^2)}{1 + \alpha} \quad (11)$$

Figure 10 shows how two cross-metathesitically interacting chains will end up after several steps at a final polydispersity of $N_w/N_n = 1.5$, and that if the starting N_w/N_n is greater than this, the polydispersity and N_w decrease during successive interactions, whereas polydispersity and N_w increase if N_w/N_n starts less than 1.5. The relationship between $N_{w,0}$ and $N_{w,fin}$ as a function of $N_{w,0}/N_{n,0}$ is shown in the inset to Figure 10.

Of course, the above treatment is merely to show the plausibility of the trends. The actual final values of polydispersity as well as the crossover masses will depend on the type of molar mass distribution involved as the cross-metathesis begins. While detailed analysis is beyond the scope of this paper, the above result can be generalized to an arbitrary starting distribution of chains $m_i = f(N_i)$, where m_i is the number of chains of length N_i . The total number of chains S is given by

$$S = \sum_{i=1}^{\infty} m_i \quad (12)$$

The number of ways S chains can be interacted two at a time, n , is

$$n = \frac{S!}{2(S-2)!} \quad (13)$$

Whence it can be shown that after averaging over every possible binary interaction in the population, the new $N_{w,f}$ after one average interaction per initial pair of chains is

$$N_{w,f} = \frac{1}{n} \left\{ \sum_{i=2}^{\infty} \sum_{j=1}^{i-1} m_i m_j \frac{1}{2(N_i + N_j)} \left[\frac{5}{3} (N_i^2 + N_j^2) + 2N_i N_j \right] + \sum_{i=1}^{\infty} \frac{m_i!}{2(m_i - 2)!} \frac{16}{3} N_i \right\} \quad (14)$$

This form is helpful for discrete distributions, such as the Poisson chain length distribution often considered appropriate to living reactions. Here, the second term on the right represents chains of the same length undergoing cross-metathesis, and it is 0 if $m_i = 1$. More importantly, in the limit of a large

population of chains the second term is negligible compared to the first term. In the limit of $m_i \gg 1$ for all i , and treating the chain length as a continuous variable x , the left-hand term can be integrated to yield

$$N_{w,f} \approx \frac{2}{S^2} \left\{ \int_0^{\infty} \int_0^y \frac{m(x) m(y)}{2(x+y)} \left[\frac{5}{3} (x^2 + y^2) + 2xy \right] dx dy \right\} \quad (15)$$

This integral can be difficult to evaluate in closed form for common distributions, such as the log-normal distribution. The simplest, albeit not typically realistic, distribution is that $m(x) = \text{constant}$ from $x = 0$ up to some finite value of chain length. In this case, the starting $M_w/M_n = 4/3$, and the integral above can be evaluated, with the final result that $M_w, M_{n,final} = 4/3$; i.e., this shows that the value of $N_w/N_n = 1.5$, appropriate for the case of just two chains, is not a general result and that the final value will depend on the details of the initial distribution. In the case of $m(x) = \text{constant}$, cross-metathesis does not change the polydispersity. We expect, however, the basic principle illustrated above to hold; for any given initial distribution, there will be a final, equilibrium distribution, whose N_w and final polydispersity may be higher or lower than the initial polydispersity, which can be evaluated by the above expression.

Conclusions

ACOMP allows a comprehensive characterization of ROMP reactions in terms of monomer conversion kinetics, and evolution of M_w and $[\eta]_w$, and is a unique tool for investigating varying reaction conditions and seeking effects such as termination and degradative mechanisms. The primary conversion phase is first order, with near linear increase in M_w with conversion, as expected for living polymerization, and target masses are obtained for NAc, but not for COD.

There is often a second phase where M_w decreases, which is highly dependent on the monomer used and its concentration. A preliminary analysis suggests this is due mostly to cross-metathesis, in which M_w and M_w/M_n should decrease for "high" starting polydispersity, but both M_w and M_w/M_n should increase for low starting M_w/M_n . It is suggested that for p(COD) the fact that molar masses are far below target values after the fast conversion phase implies a fast intramolecular reaction, such as backbiting that leads to chain transfer and high polydispersity. The large decreases in M_w during the second phase are due to cross-metathesis.

Cross-checks by conventional multidetector GPC on manually withdrawn aliquots were found to be in excellent agreement with the ACOMP results and also show the high polydispersity for p(COD).

This work is a first step in applying ACOMP to the precise control and production of highly tailored polymers, including copolymers of different architectures. A further near term goal is to use ACOMP to monitor and quantify the wide variety of postpolymerization processes that can be used to functionalize polymers produced by ROMP and to monitor diblock and alternating copolymerization reactions.

Acknowledgment. The Tulane authors acknowledge support from NSF CTS 0623531, NASA NCC3-946, and La. BoR RD-B-7. Support for the UMass authors and central analytical facilities was made available through the NSF-supported Materials and Research Science and Engineering Center on Polymers at UMass Amherst (DMR-0213695). All the Tulane authors were displaced from New Orleans in August 2005 due

to Hurricane Katrina. They thank the Polymer Science & Engineering Dept. at U. Massachusetts at Amherst, for the warm welcome extended to them in Katrina's aftermath. The current work was carried out at U. Massachusetts, and the authors further thank the following entities for generous help in terms of loans and equipment donations: Shimadzu Inc., Polymer Laboratories Inc., and Brookhaven Instruments Corp. The authors also acknowledge Tulane's permission to temporarily relocate some of the Tulane ACOMP instrumentation to U Mass.

References and Notes

- (1) Grubbs, R. H. *Handbook of Metathesis*; John Wiley: New York, 2003.
- (2) Grubbs, R. H. *Tetrahedron* **2004**, *60*, 7117.
- (3) Baughman, T. W.; Wagener, K. B. *Adv. Polym. Sci. Springer* **2005**, *176*, 1.
- (4) Buchmeiser, M. R. *Chem. Rev.* **2000**, *100*, 1565.
- (5) (a) Chauvin, Y. *Angew. Chem., Int. Ed.* **2006**, *45*, 3740. (b) Schrock, R. R. *Angew. Chem., Int. Ed.* **2006**, *45*, 3748. (c) Grubbs, R. H. *Angew. Chem., Int. Ed.* **2006**, *45*, 3760.
- (6) Rule, J. D.; Moore, J. S. *Macromolecules* **2002**, *35*, 7878.
- (7) Demel, S.; Schoefberger, W.; Slugovc, C.; Stelzer, F. *J. Mol. Catal. A* **2003**, *200*, 11.
- (8) Love, J. A.; Sanford, M. S.; Day, M. W.; Grubbs, R. H. *J. Am. Chem. Soc.* **2003**, *125*, 10103.
- (9) Sanford, M. S.; Ulman, M.; Grubbs, R. H. *Am. Chem. Soc.* **2001**, *123*, 749.
- (10) Florenzano, F. H.; Strelitzki, R.; Reed, W. F. *Macromolecules* **1998**, *7226*.
- (11) Giz, A.; Catalgil-Giz, H.; Alb, A. M.; Brousseau, J. L.; Reed, W. F. *Macromolecules* **2001**, *34*, 1180.
- (12) Chauvin, F.; Alb, A. M.; Bertin, D.; Tordo, P.; Reed, W. F. *Macromol. Chem. Phys.* **2000**, *203*, 2029.
- (13) Mignard, E.; Lutz, J.-F.; Matyjaszewski, K.; Guerret, O.; Reed, W. F. *Macromolecules* **2005**, *38*, 9556.
- (14) Farinato, R. S.; Calbick, J.; Sorci, G. A.; Florenzano, F. H.; Reed, W. F. *Macromolecules* **2005**, *38*, 1148.
- (15) Catalgil-Giz, H.; Giz, A.; Alb, A. M.; Oncul, A. K.; Reed, W. F. *Macromolecules* **2002**, *35*, 6557.
- (16) Mignard, E.; Leblanc, T.; Bertin, D.; Matyjaszewski, K.; Guerret, O.; Reed, W. F. *Macromolecules* **2004**, *37*, 966.
- (17) Grassl, B.; Alb, A. M.; Reed, W. F. *Makromol. Chem. Phys.* **2001**, *12*, 2518.
- (18) Reed, W. F. *Macromolecules* **2000**, *33*, 7165.
- (19) Choi, T.-L.; Grubbs, R. H. *Angew. Chem., Int. Ed.* **2003**, *42*, 1743.
- (20) Strelitzki, R.; Reed, W. F. *Macromolecules* **1998**, *31*, 7226.
- (21) Sorci, G. A.; Reed, W. F. *Macromolecules* **2002**, *35*, 5218.
- (22) Love, J. A.; Morgan, J. P.; Trnka, T. M.; Grubbs, R. H. *Angew. Chem., Int. Ed.* **2002**, *41*, 4035.
- (23) Reed, W. F. In *Macroion Characterization*; Schmitz, K., Ed.; American Chemical Society: Washington, DC, 1994.
- (24) Reed, W. F.; Reed, C. E. *J. Chem. Phys.* **1991**, *93*, 8479.
- (25) Bielawski, C. W.; Grubbs, R. H. *Angew. Chem., Int. Ed.* **2000**, *39*, 2903.
- (26) Ivin, K. J.; Mol, J. C. *Olefin Metathesis and Metathesis Polymerization*; Academic Press: San Diego, CA, 1997; pp 368–374.

MA062241I